Space Station Freedom Solar Array Wing: Nonlinear Transient Analysis of Plume Impingement Load

C. C. Tang
Structural Dynamist, Space System Division
Lockheed Missile & Space Company
Sunnyvale, California

Abstract

This paper describes the nonlinear transient analysis of the Space Station Freedom Solar Array (SSFSA) wing for on-orbit plume impingement load due to Space Shuttle berthing. Design features and the finite element model of the SSFSA wing are briefly described. Nonlinear transient analysis is performed using MSC/NASTRAN SOL 99 (V67) with blanket tensioning accomplished by restarting with static solution results. The blanket tensioning is from tension mechanisms. Transfer function (TF), scalar point (SPOINT), nonlinear load (NOLIN1), and damper (CDAMP2) are used to describe the nonlinear characteristics of the tension mechanisms. Stiffness updates for capturing the nonlinear geometrical stiffness changes due to tension variation in the solar array blankets is utilized in the iterative nonlinear solution. Results, when compared to that from linear transient analysis, showed that the beam-column effect for the slender mast of the solar array wing is insignificant, and the assumptions made in the linear transient analysis are acceptable.

1.0 Introduction

The Space Station Freedom Solar Array (SSFSA) wing is the largest solar array that has ever been designed for a spacecraft. The structural design of its mast and blanket assemblies, are dictated by on-orbit plume impingement load due to the Space Shuttle. To meet minimum frequency requirements of 0.10 hertz, 150 pounds of tension is applied to the blankets. This tension induces axial compression in the long slender mast. Mast bending moment caused by beam-column (or p-delta) effect during plume impingement needs to be assessed. In order to accurately evaluate this effect, nonlinear transient analysis is performed using MSC/NASTRAN SOL 99 (Ref. 1) with blanket tensioning accomplished by restarting with static solution results. The blanket tensioning is from tension mechanisms. Transfer function (TF), scalar point (SPOINT), nonlinear load (NOLIN1), and damper (CDAMP2) are used to describe the nonlinear characteristics of the tension mechanisms. Stiffness updates capturing the nonlinear geometrical stiffness changes due to tension variation in the solar array blankets is utilized in the iterative nonlinear solution. Results, when compared to that from linear transient analysis, showed that the beam-column effect for the slender mast of the solar array wing is insignificant, and the assumptions made in the linear transient analysis are acceptable.

The solar array wing is part of the electrical power system, also known as WP-04, for the Space Station Freedom (SSF) program. NASA Lewis Research Center (LeRC) is field center responsible for WP-04. Rocketdyne (RD) is the prime contractor. LMSC is the subcontractor responsible for the design, analysis, and manufacture of the SSFSA wing. AEC-Able Engineering is a subcontractor to LMSC, providing the mast/canister subassembly for the SSFSA.

2.0. Description of Solar Array Wing

The SSFSA wing is a dual flexible solar blanket design which converts solar energy to electricity for the SSF operation. The SSFSA wing consists of mast/canister assembly, tip fitting, pivot fittings, containment box assembly, blanket assembly, tension mechanism, and guidewire mechanism. During launch, the SSFSA wing is in a stowed configuration. During on-orbit blanket deployment, first, the containment box cover is unlatched from the containment box base. Secondly, the stowed mast extends out of the canister, pulling the containment box cover away from the containment box base, and unfolding the stowed blanket panels. Figure 1 shows the SSFSA wing in a partially deployed configuration with first few bays of the mast extended. When the mast is fully extended and all the blanket panels are open along the guide wires, the two tension mechanisms apply an average tension of 75.0 pounds to each blanket assembly. Figure 2 shows the on-orbit fully deployed SSFSA wing.

The fully extended mast is a 1296 inch long truss-like boom structure. It consists of aluminum longerons, fiberglass battens, steel cable diagonals, elbow fittings, and corner fittings. Each blanket assembly consists of 2 inactive leading panels and 82 active panels. Each active panel consists of 0.0035 inches laminate with E-glass and kapton. Solar cells are bonded to one side. The size of each panel is 14.9 inches by 170.0 inches. The inactive panel is laminate only. The panels are connected together using hinge pins along their long sides. The top leading panel is attached to containment box cover through 161 top edge springs. The bottom leading panel is attached to top

side of the tension distribution bar through 161 bottom edge springs. Tension is applied to the blanket plane through two tension mechanism tension wires, attached to bottom side of the tension distribution bar. The tension mechanism has a power spring inside the tension mechanism housing, which is mounted on the under side of the containment box base. Proper combination of soft top edge springs, soft bottom edge springs, stiff tension distribution bar, and stiff containment box cover is chosen to ensure that the entire blanket assembly is in tension. There are three guide wires for each blanket assembly. Each guide wire has a tension of 1.0 pound, provided by the negator spring of the guidewire mechanism, which is also mounted on under side of the containment box base. Every other panel of the blanket are connected to the guide wires through grommets. The guide wires guide and provide lateral stability for unfolding and folding of the blanket panels during wing deployment and retraction. Tension mechanisms and guidewire mechanisms have extra spring length to allow free movement of the blanket assembly from its normal position due to temperature changes and plume impingement. The base of the canister is attached to a beta gimbal on the SSF main truss. The weight of the SSFSA wing is approximately 2200 pounds.

3.0 Finite Element Model Description

The MSC/NASTRAN finite element model of the fully deployed SSFSA wing is shown in Figure 3. The origin of the coordinate is chosen at center of the canister base. The Z axis is along the mast and canister longitudinal axis pointing toward mast tip. The X axis is normal to the blanket plane. The Y axis, determined using right hand rule, is parallel to the containment box cover and base.

The canister and the mast are modeled using beam elements with equivalent sectional properties verified by static test. The compliance between the mast and canister is idealized using spring elements. The remaining structural members, such as containment box covers, containment box bases, pivot fittings, tip fitting, and tension distribution bars, are also modeled using beam elements. The blanket panels are represented by triangular membrane elements. The hinge pins between blanket panels are modeled using beam elements. The one dimensional top and bottom edge springs are modeled using rod elements. The tension wire of the tension mechanism is also modeled using rod elements. At the lower end of each tension wire, two coincident grids are used to represent the lower end point of the tension wire in normal position and the mounting point of the tension mechanism on the containment box base. The two coincident grids are tied together in the lateral directions of the tension wire, but are able to move independently in the longitudinal (z direction) of the tension wire. This method of modeling captures the salient tension mechanism design feature that the tension wire can payout and payin with nearly constant tensile force. The tension force in the tension wire of the tension mechanism is represented by a pair of opposite forces applied to the two coincident grids. Further discussion of the tension force due to the tension mechanism is given in Section 4.0.

To reduce the size of the problem to be solved, the guide wires are neglected in the finite element model for the analysis presented herein, since its contribution to SSFSA wing dynamic response is insignificant.

The weight of the SSFSA wing is modeled using material density, non-structural weight, and lumped weight at selected grids.

4.0 Analysis Approach

Plume impingement loading

The plume impingement load case chosen for the analysis is due to Norm Z-Jet firing for the normal z break-out of the Space Shuttle. This load case (259) is one of three load cases generated by NASA/LeRC. The temporal distribution of this load case, which is an impulse of 1.28 second duration, is given in Figure 4. The RCSFORCE program (Ref. 3) is used to compute the spatial force distribution on blanket grids due to the plume impingement. This plume impingement load case is selected for this study because: (a) It produces mast internal loads comparable to the design value; and (b) The mast responses reach maximum values in the first few second of the transient solution, providing significant cost saving in the nonlinear transient analysis.

A normalized shock spectra plot of this load case is shown in Figure 5. It reveals that the dynamic response would be very sensitive to variation of structural frequencies below 0.37 hertz. The SSFSA wing has significant structural modes below 0.37 hertz.

Linear transient analysis

The linear transient analysis is based on a modal solution. A similar approach is also used to represent the SSFSA wing in the SSF system level on-orbit coupled loads analysis for plume impingement loading.

The linear analysis assumptions are:

- The blanket tension remains constant, and is not affected by plume impingement on the blanket.
- Secondary beam-column effect for the slender mast is not considered in the transient analysis.
- The pre-stressed status of the wing does not affect the dynamic response of the wing components during the plume impingement.

The linear transient analysis of the SSFSA wing for plume impingement loading are carried out using the following steps:

(1) Geometric nonlinear static analysis using SOL 66 (or SOL 64) -- Without tensioning, the blanket assembly does not posses lateral stiffness. In order to account for the tension stiffening effect of the blanket panels, top edge springs, bottom edge springs, and tension wires, geometric stiffness must be computed for these elements (Ref. 4). The SSFSA wing is analyzed for a nominal tension load of 75.0 pounds for each blanket (37.5 pounds from each tension mechanism). Large displacement and follower force options are used to achieve accurate non-uniform stress distribution in the blanket. The final converged solution provides the system

stiffness matrix that includes both the conventional structural stiffness and the geometric stiffness.

(2) Normal mode solution -- SOL 63 is used to determine the SSFSA wing modal frequencies based on the system stiffness matrix saved in step (1) above. The first modal frequency of the wing is 0.10 hertz. This mode is the blanket out-of-plane bending mode, and is dictated by the magnitude of tension in the blanket. The frequencies of the dominant modes are from 0.10 hertz to 0.20 hertz.

(3) Modal transient solution -- The response of the SSFSA wing subjected to plume impingement load is performed using SOL 72. The modal data saved in step (2) is used in this solution. A modal damping ratio of 0.02 is used for the SSFSA wing based on past experience (Refs. 2 & 5). All modes with frequency less than 10 hertz are included in the solution.

(4) Combination of results -- In order to obtain the total component stress due to blanket tension and plume impingement loads, the results from steps (1) and (3) are added together.

As an alternative, LMSC has developed user DMAPs and a post processing program to perform steps (2) to (4). In addition, these DMAPs can also handle application of base shake accelerations.

Nonlinear tension mechanism

Development tests of the tension mechanism design showed that the tension provided by the power spring has nonlinear characteristic. The tension varies according to the power spring stroke position and whether the tension wire is paying out or paying in. The modeling of the nonlinear tension mechanism in MSC/NASTRAN SOL 99 is accomplished by the following procedures:

(1) The power spring stroke is established by defining a transfer function (TF), which associates a scalar point with the relative displacement of the two coincident grids at the lower end of the tension wire. The relative displacement relation is expressed as:

$$s_1 = uz_a - uz_b$$

This relation is also defined by a multi-point constraint (MPC) equation in SOL 66, in order to pass the proper initial condition into SOL 99 and to make the model data base compatible for restart (SOL 66 does not accept transfer function definition for K2PP matrix).

(2) The power spring force of the tension mechanism is expressed as:

$$F_{tot} = F_{avg} + F_{non}(s_1)$$

F_{avg} is the average tension force of 37.5 pounds for the power spring. F_{non} equals the difference between the total tension force and the average tension force of the power spring. F_{avg} remains constant and is treated as follower force (following the direction of tension wire) in SOL 99. F_{non} is a function of the scalar point (s_1) displacement, and is defined as nonlinear

force (NOLIN1) using piece wise linear tabulated values. Using this approach, only a small portion of the tension mechanism tension is treated as nonlinear force in the solution; thus, the numerical iteration is greatly improved.

(3) Past experience (Refs. 2, 5 & 6) indicated that the hysteresis loop provided by the nonlinear tension mechanism gives additional damping for solar array blanket in-plane modes. To represent this effect, the Voigt model (Ref. 7) is used to derive a dashpot damper for the tension mechanism. The damping coefficient is computed as:

$$c = \frac{E}{\pi \omega D^2}$$

E is the energy dissipated by the hysteresis loop per cycle. ω is the dominant frequency. D is the displacement. ω and D are obtained from the linear transient response result at the lower end of the tension wire. The damper (CDAMP2) is connected to the two coincident grids at the lower end of the tension wire.

Nonlinear transient analysis

Nonlinear transient analysis is performed for the purpose of:

- Verifying the linear transient analysis results are indeed valid for this unique and unconventional structure.
- Evaluating beam-column effect for the long slender mast.
- Evaluating the effect of the nonlinear tension mechanism.

The nonlinear transient analysis of the SSFSA wing for blanket tension and plume impingement loading are carried out in the following two steps:

(1) Geometric nonlinear static analysis using SOL 66 -- This analysis step is the same as that for the linear transient analysis described earlier. However, the entire converged solution status is saved for restarting into SOL 99.

(2) Direct time integration solution using SOL 99 -- Using SOL 66 results as the initial displacement condition due to blanket tension, nonlinear transient analysis of the wing is performed using SOL 99. The applied loads are from plume impingement, and tension mechanisms, which are nonlinear. SOL 99 uses the Newmark Beta numerical integration method and the modified Newton iteration to ensure convergence between the integration steps. The solution strategy is:

- Set up the entire solution run in several subcases for better control of integration time step sizes. The time step sizes used for the analysis varies from 0.002 seconds to 0.01 seconds.
- Convergence criterion is based on both load equilibrium error tolerance and work error tolerance.

- Update stiffness matrix every 2 to 4 time steps in order to capture the stiffness change in the blanket elements due to tension variation. This also reduces the number of iterations required to achieve convergence.
- Use proportional damping equivalent to 2.0 percent critical damping for the dominant mode.
- Use large displacement and follower force (for tension mechanism tension only) options.
- Use restart option in SOL 99 between the subcases such that satisfactory solution result is assured before carrying out the solution further.

5.0 Analysis Results and Discussions

The linear transient analysis is performed for 20 seconds. For cost saving, the nonlinear transient analysis is carried out to 8 seconds. The peak responses of the mast from both analyses are given in Table 1 for comparison. Also provided in the Table 1 are times when peak responses occur and the percent difference for the peak response. Selected response plots from the nonlinear transient are provided in Figures 6 through 10. Comparison of the mast response showed:

- Longeron axial load, induced by combined action of the mast axial force and bending moments, from nonlinear transient is slightly less than that from linear transient. This indicates that the beam-column effect for the mast during plume impingement is insignificant.
- Absolute maximum of the mast shear and torsion from the nonlinear transient is more than that from the linear transient analysis.
- The response trends from both analyses are quite similar. However, some peak responses occur at different times, indicating a shift of system frequencies, caused by stiffness change and additional damping, in the nonlinear transient.
- The maximum difference of peak response for the mast base X direction shear is 21.9 percent, probably on the high end of what is normally considered acceptable in engineering practice. The large difference may be caused by the response sensitivity to frequency change below 0.37 hertz (see Figure 5).

The tension wire axial stress from the nonlinear transient analysis is plotted in Figure 10 for one of the outer tension mechanism. The tension wire axial stress varies from 19.37 ksi to 24.12 ksi, which correspond to an axial force variation of 33.50 pounds to 41.73 pounds. For the linear transient analysis, the tension wire axial force is assumed to remain at 37.5 pounds. The plot also showed that the integration time step size chosen is adequate for the localized, relatively high frequency component response.

The analyses were carried out on Cray Y-MP computer using MSC/NASTRAN Version 67. For the nonlinear transient analysis, the model has 3008 degrees of freedom. Computer time for 8 seconds of nonlinear analysis is 400 sec. system cpu and 7500 sec. user cpu.

6.0 Conclusions

Results of this plume impingement study demonstrated that:

- The beam-column effect for the slender mast is negligible.
- The assumptions made in the linear transient analysis are indeed valid.

7.0 Acknowledgments

The author wishes to thank: Farhad Nekoogar for contributions to finite element modeling and preliminary test runs; Gary Goble for setting up linear transient analysis DMAPs; and A. J. Elliott and Charles Shih for their constructive comments and suggestions. Appreciation is also due to Isam Yunis and Damian Ludwiczak (both with NASA/LeRC) for developing the plume load case input, and numerous engaging conversations on beam-column effects and plume load analysis.

8.0 References

[1] MSC/NASTRAN User's Manual, Version 67, The MacNeal-Schwendler Corporation, Los Angeles, CA, August 1991.

[2] Lockheed Missile and Space Co., "Solar Array Flight Experiment Final Report", Report No. LMSC-F087173, Marshall Space Flight Center Contract No. NAS-8-31352, April 1986.

[3] Rayos, E. M. (Lockheed Engineering and Science Co.), "RCSFORCE Program", modified by NASA/LeRC, Version 5.

[4] Clough, R. W. and Penzien, J., Dynamics of Structures, 1st edition, McGraw-Hill, 1975.

[5] Young, L. E. and Pack, Jr., H. G., "Solar Array Flight Experiment/Dynamic Augmentation Experiment", NASA Technical Paper 2690, February 1987.

[6] Pinson, E. D., "Discrete Mechanism Damping Effects in the Solar Array Flight Experiment", 20th Aerospace Mechanisms Symposium, NASA/Lewis Research Center, Cleveland, OH, May 7-9, 1986.

[7] Thomson, W. T., Theory of Vibration with Application, 2nd edition, Prentice-Hall, 1972.

Table 1. Mast Peak Response Comparison

Item description	Nonlinear transient		Linear transient		Magnitude [1] percent difference
	Magnitude	Time (sec.)	Magnitude	Time (sec.)	
Mast base [2] longeron axial load	-338.5 lbs [3]	2.37	-351.0 lbs	2.40	+3.59
Mast base x shear	8.07 lbs	7.19	6.62 lbs	7.61	-21.90
	-5.97 lbs	3.40	-5.85 lbs	3.39	-2.05
Mast base y shear	7.95 lbs	5.27	8.13 lbs	5.92	+2.21
	-10.39 lbs	1.80	-9.44 lbs	2.33	-10.06
Mast base torsion	279.7 in-lbs	7.03	271.8 in-lbs	6.62	-2.91
	-299.1 in-lbs	2.84	-258.4 in-lbs	3.00	-15.75
Mast tip x displacement	5.71 in	3.64	5.46 in	3.63	-4.58
	-4.87 in	7.42	-3.98 in	7.39	-22.36
Mast tip y displacement	6.33 in	2.18	6.92 in	2.26	+8.53
	-4.83 in	5.32	-6.08 in	5.49	+20.56

Notes:

(1) Magnitude percent difference is defined as linear transient result minus nonlinear transient result, then divided by linear transient result and times 100.

(2) Longeron axial load represents combined action of mast bending moments and mast axial force.

(3) Value corresponding to a compressive stress of 1110.11 psi for the equivalent beam section of the mast.

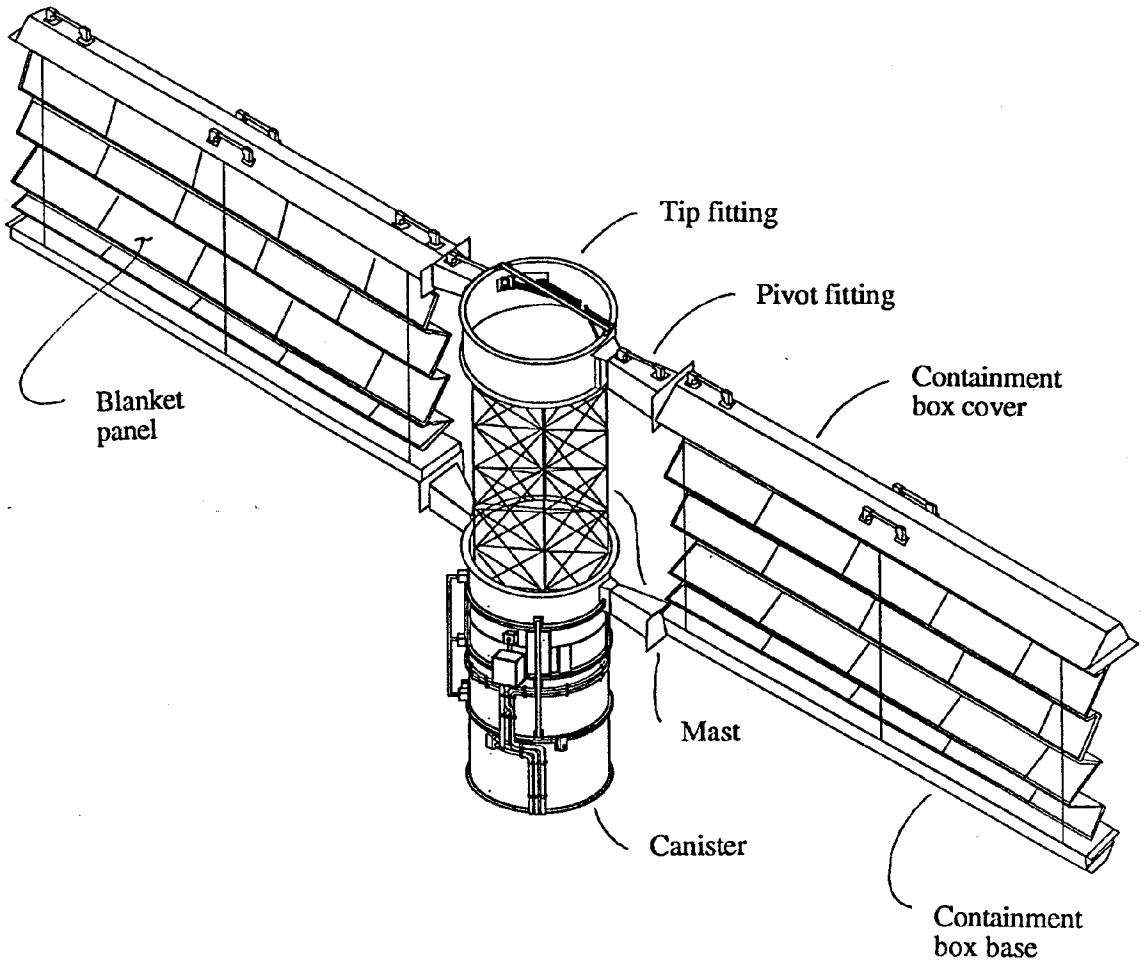

Figure 1. Solar array wing in partially deployed configuration

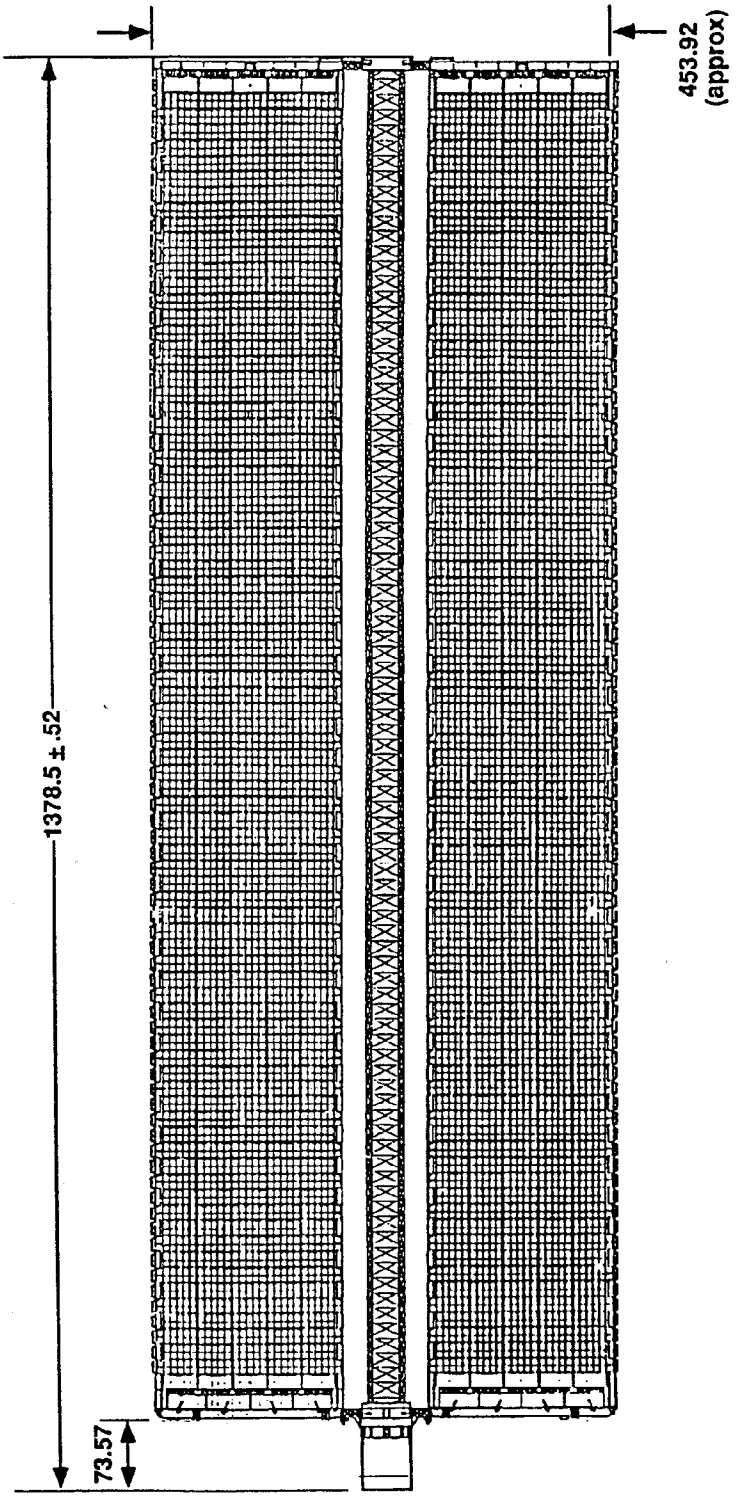

Figure 2. Solar array wing in fully deployed configuration

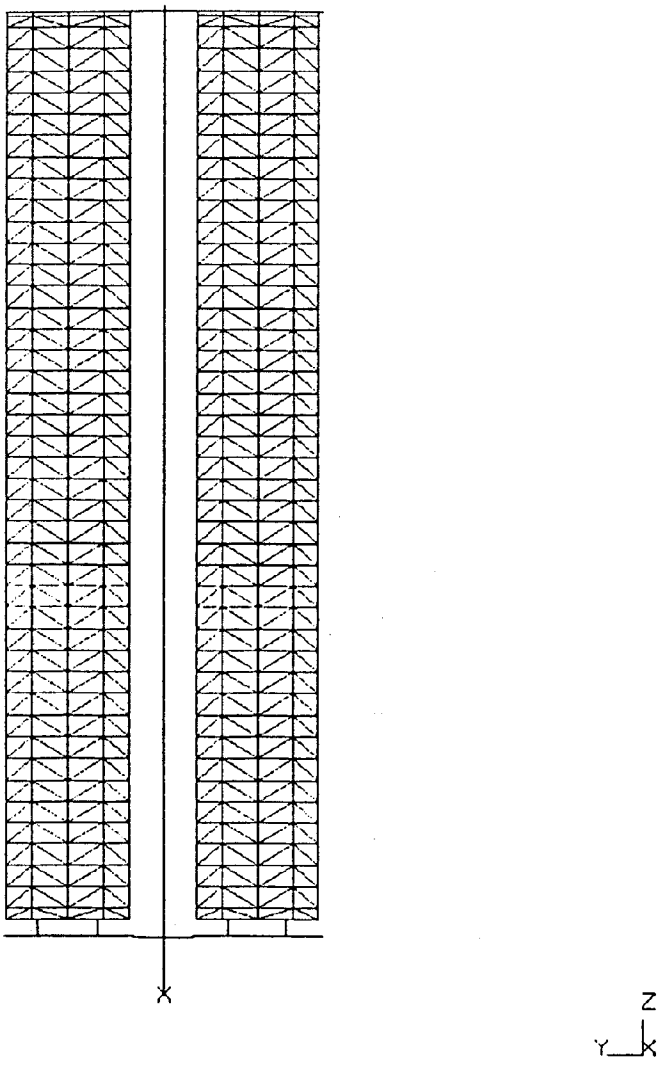

Figure 3. Solar array wing finite element model

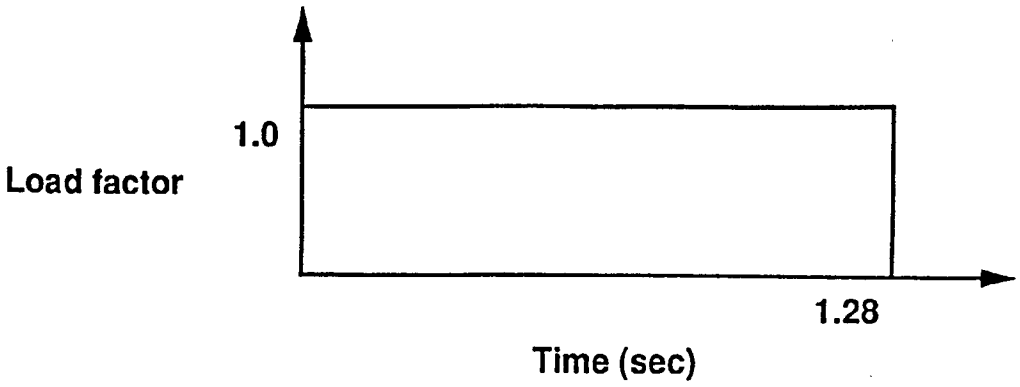

Figure 4. Plume impingement forcing function
(NASA/LeRC load case 259)

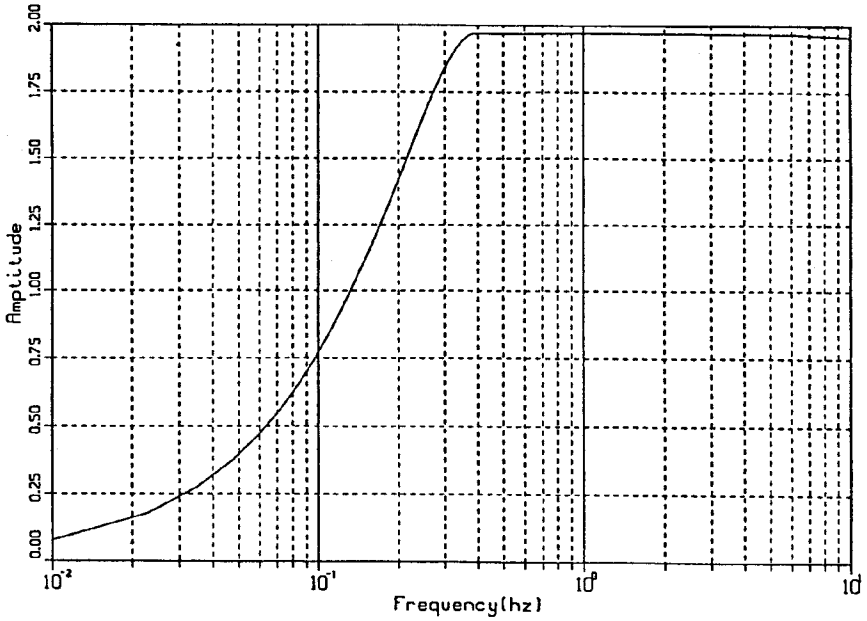

Figure 5. Normalized shock spectra of plume load

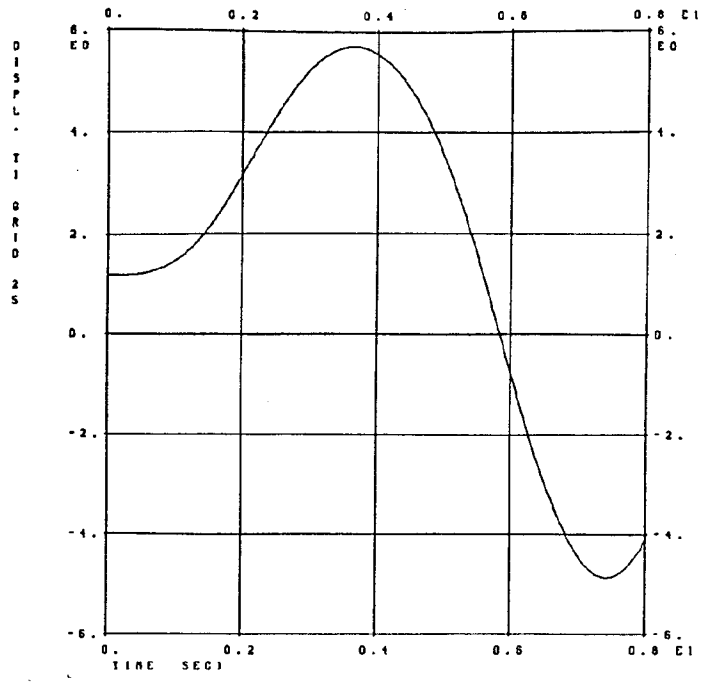

Figure 6. Mast tip x displacement

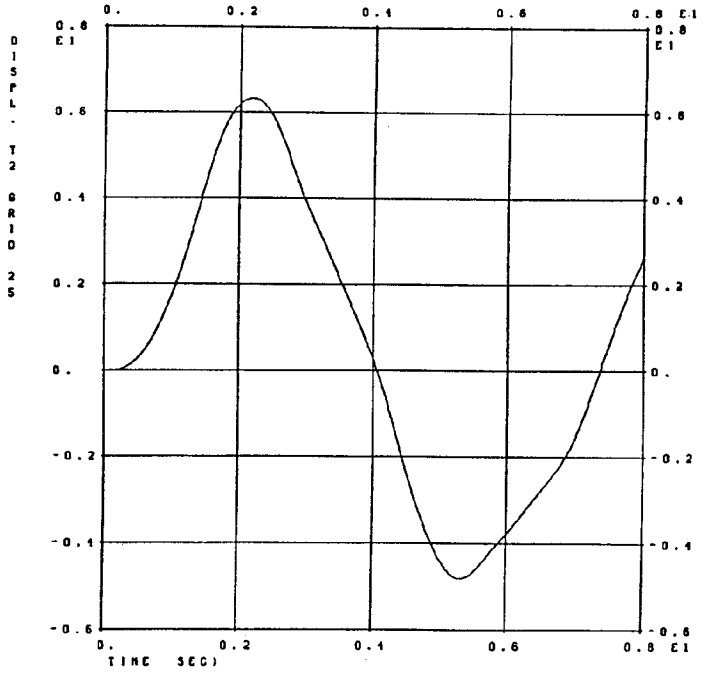

Figure 7. Mast tip y displacement

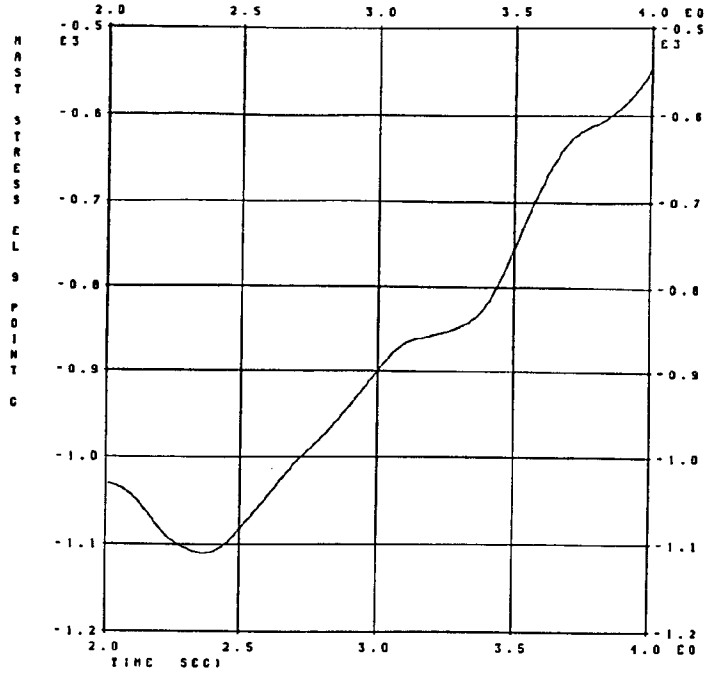

Figure 8. Mast longeron equivalent stress

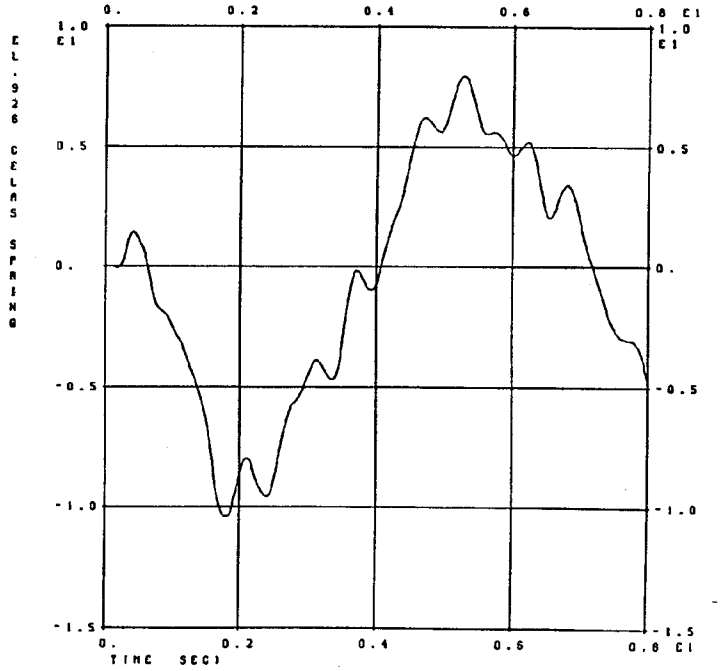

Figure 9. Mast base y shear

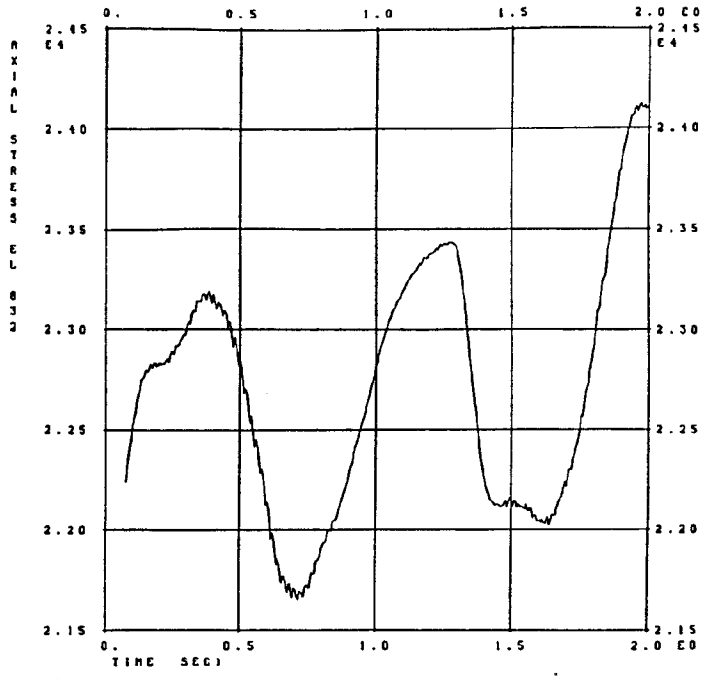

Figure 10. Tension wire axial stress

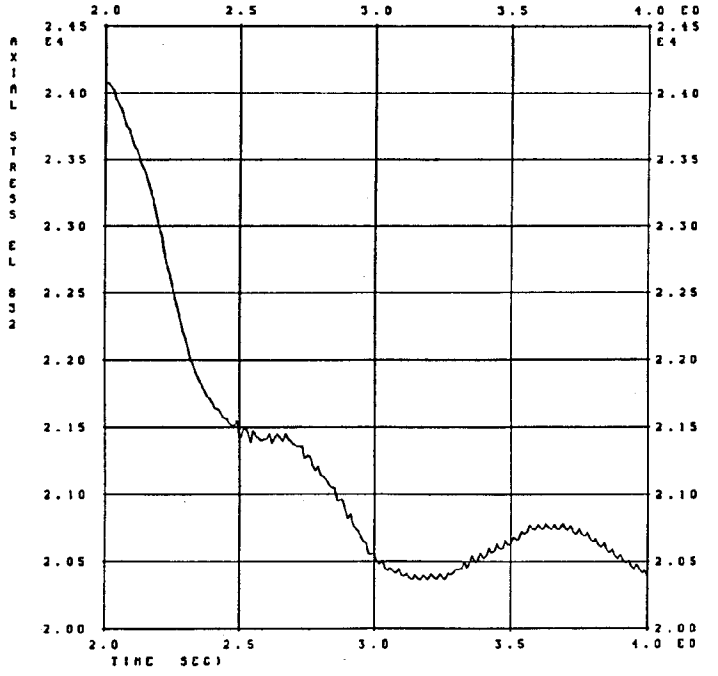

Figure 10. Tension wire axial stress (continued)

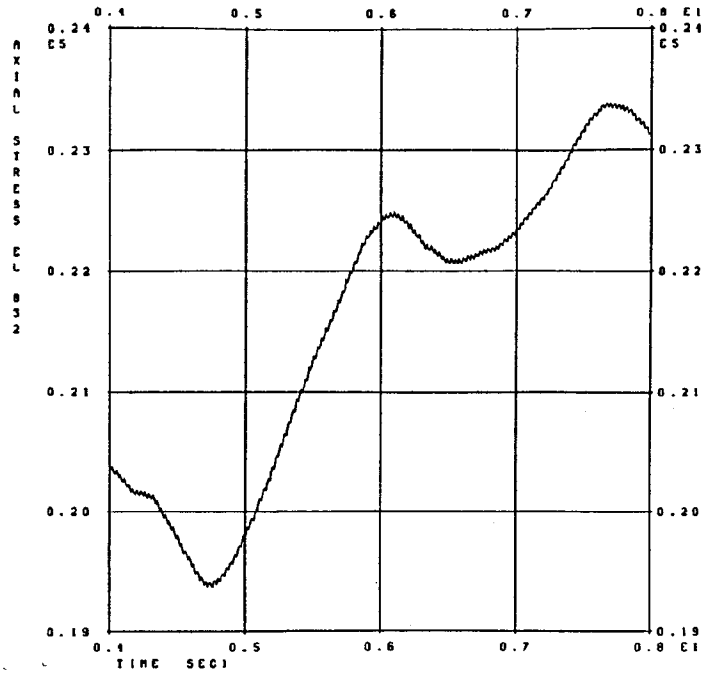

Figure 10. Tension wire axial stress (continued)